

Deuterium retention in tungsten under combined high cycle ELM-like heat loads and steady-state plasma exposure



A. Huber^{a,*}, G. Sergienko^a, M. Wirtz^a, I. Steudel^a, A. Arakcheev^b, S. Brezinsek^a,
A. Burdakov^b, T. Dittmar^a, H.G. Esser^a, M. Freisinger^a, A. Kreter^a, J. Linke^a, Ch. Linsmeier^a,
Ph. Mertens^a, S. Möller^a, M. Reinhart^a, A. Terra^a, B. Unterberg^a

^a Forschungszentrum Jülich GmbH, Institut für Energie- und Klimaforschung, 52425 Jülich, Germany,

^b Budker Institute of Nuclear Physics (BINP), Novosibirsk 630090, Russia

ARTICLE INFO

Article history:

Received 26 November 2015

Revised 21 March 2016

Accepted 11 April 2016

Available online 16 May 2016

PACS:

28.52.-s

28.52.Fa

52.40.Hf

65.40.De

68.43.Vx

78.70.-g

Keywords:

Transient heat loads

Deuterium retention

Blistering

Surface modifications

Tungsten

ABSTRACT

To investigate the synergistic effects of fuel retention in tungsten, experiments were performed in the linear plasma device PSI-2 where the transient heat loads were applied by a high energy laser during the steady-state plasma operation. The impact on the deuterium (D) retention of simultaneous and sequential exposures to laser and plasma has been investigated. A significant increase of D retention, more than a factor of 12, has been observed during the simultaneous transient heat loads and plasma exposure. Successive exposures to transient heat loads and deuterium plasma also show the increased content of D-atoms by more than a factor of 3.6 in comparison to the pure plasma loading. In both cases the increase is most likely due to enhanced hydrogen clustering by the thermal shock exposures, due to an increased mobility of D atoms along the shock-induced cracks as well as to increased diffusion of D atoms into the W material caused by strong temperature gradients during the laser pulse exposure.

Comparison of the NRA and TDS measurements shows that only 34% of the retained deuterium in the tungsten specimen is located inside the near-surface layer ($d < 4 \mu\text{m}$) after simultaneous as well as sequential exposures of W to heat load.

Enhanced blister formation has been observed under combined loading conditions at power densities close to the threshold for damaging. It is shown that blisters are not mainly responsible for the pronounced increase of the D retention.

© 2016 The Authors. Published by Elsevier Ltd.

This is an open access article under the CC BY license (<http://creativecommons.org/licenses/by/4.0/>).

1. Introduction

Tungsten (W) is foreseen as the main plasma-facing material (PFM) in fusion devices, such as ITER with full-tungsten divertor [1,2], because of its excellent material properties such as a high threshold energy for sputtering [3], a high melting point [4] and a low tritium inventory [5,6]. The hydrogen isotope retention in tungsten is not a critical issue and is generally considered to be small, but it can be strongly raised during intense transient events such as Edge Localised Modes (ELMs), causing surface modifications and damages or even melting of plasma-facing components (PFC). Despite substantial efforts to quantify hydrogen retention in tungsten, not all underlying mechanisms responsible for the behaviour of implanted hydrogen isotopes in W are fully understood yet. In particular, the influence of synergistic effects of combined

high cycle ELM-like heat loads and steady-state plasma exposure can lead to a significantly increased material damage during transients as well as to a significant impact on fuel retention in the PFCs. The combination of transient heating and hydrogen plasma exposure has been experimentally shown to lead to severe surface damage and modifications, such as crack formation, enhanced erosion/ejection, roughening, formation of melt layers and blisters [7–9]. These results show that the damage behaviour strongly depends on the loading conditions and the sequence of the particle and heat flux exposure. Additionally, the neutron-induced damage may act as a trap site for hydrogen leading to the increase of the tritium retention. The effects of neutron damage on the retention of tritium in the PFC are beyond the scope of this paper.

Therefore, a detailed study of the synergistic effects of these combined loading conditions on the damage behaviour as well as on the fuel retention of tungsten is necessary to qualify tungsten as plasma-facing material (PFM).

* Corresponding author. Tel.: 00441235464809.

E-mail addresses: A.Huber@fz-juelich.de, a.huber@fz-juelich.de (A. Huber).

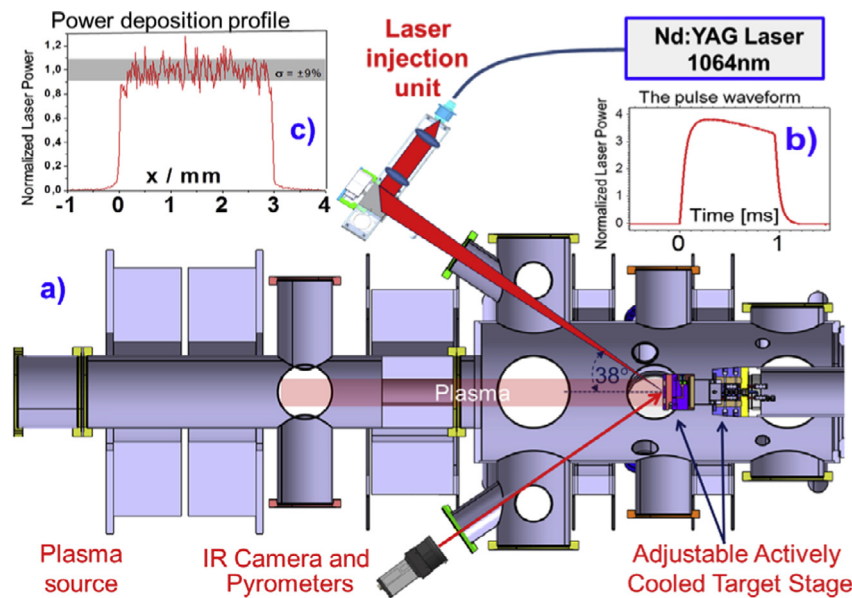


Fig. 1. PSI-2 layout including the target station and laser irradiation set-up with a laser pulse waveform and the spatial distribution of the laser energy over the irradiated spot.

However, in addition to the transient heat loads, there will be an enhanced particle flux during the ELM events expected in ITER [10]. The additional impact of the enhanced particle flux during the ELMs is outside of the scope of this work. In this contribution, we investigate the effect of the simultaneous exposure of tungsten to steady-state plasma and transient heat loading conditions on the surface modification of bulk tungsten as well as on the fuel retention.

2. Experimental set-up

In order to investigate the synergistic effects, experiments were performed in the linear plasma device PSI-2 (Fig. 1) where the transient heat loads were applied by a high energy laser during the steady-state plasma operation. The PSI-2 device is a steady-state, linear plasma device [11] which generates plasma by an arc discharge between a heated LaB_6 cathode emitter, to which a negative voltage is applied, and a hollow molybdenum anode at ground potential. An axial magnetic field of 0.1 T confines the plasma on the axis of the vacuum chamber in form of a 2.5 m long column of about 6 cm diameter. The working gas used in these experiments was deuterium with typical plasma densities $n_e = 10^{18} - 10^{19} \text{ m}^{-3}$ and electron temperatures in the range $T_e = 1 - 20 \text{ eV}$.

Radial profiles of electron density and temperature were measured by a movable Langmuir double probe installed at the top of the target exposure chamber. The probe moved radially with a velocity of 15 mm/s, while the I - V characteristic was scanned with a frequency of 100 Hz. The radial resolution of the measurements is given by the size of the probe tips of 1.5 mm.

Targets were mounted on an adjustable actively cooled target stage of PSI-2, immersed in one end of the plasma column, and placed in the region with maximal deuterium ion flux. The sample radii during these experiments were $\approx 2.0 \text{ cm}$ and $\approx 2.7 \text{ cm}$ for the laser spot locations 1 and 2 correspondingly. The temperature of the samples was measured by a Ni-NiCr (type K) thermocouple that was connected to the rear part of the sample. Additionally, monitoring of the surface temperature has been performed by a fast pyrometer. During these experiments the target temperatures were in the range between 20°C (the base temperature of the test samples) and 130°C (the maximum temperature reached during the combined laser and plasma exposures). Ions were accelerated

to the sample surface by biasing the sample to reach an ion energy of 60 eV at a flux of about $6 \times 10^{21} \text{ m}^{-2} \text{ s}^{-1}$. Since PSI-2 is operated under steady-state conditions, the required particle fluence of $1.2 \times 10^{25} \text{ m}^{-2}$ was accumulated in a single plasma exposure for a time period of 2000 s.

Pulsed laser irradiation is used in these experiments for the simulation of the transient heat loads in fusion plasma. In these experiments, a Nd:YAG laser ($\lambda = 1064 \text{ nm}$) with maximal energy per pulse of up to 32 J and duration of 1 ms was used to irradiate tungsten samples with repetitive heat loads. The laser was operated in the free generation mode (without Q-switching) and laser pulses at the frequency of 0.5 Hz were utilised in the current contribution. The laser beam is coupled into a 600 μm quartz fibre and is introduced by a laser injection unit, through a vacuum window to the target surface at incident angle of 38° . The irradiation area was limited to a small spot size of $\varnothing 3.1 \text{ mm}$ and the power deposition profile in the irradiated area was nearly uniform (see Fig. 1c) to avoid the instrumental influence on the cracking behaviour.

The scan of the laser spot over the sample surface was performed by adjustment of the last mirror just in front of the vacuum window. In the presented experiments the samples have been exposed to ELM relevant power densities between 0.19 GW/m^2 and 0.86 GW/m^2 . Maximal heat loads expressed using heat flux factor $P \times t^{1/2}$, which is directly proportional to the surface power load multiplied by square root of pulse duration, was in our experiments $28.5 \text{ MW m}^{-2} \text{ s}^{1/2}$, that is, below the melting threshold for bulk tungsten ($54 \text{ MW m}^{-2} \text{ s}^{1/2}$).

The pulse waveform was measured by fast photodiode located behind the last dielectric mirror, shown in Fig. 1a, demonstrating the nearly constant power (Fig. 1b) during the pulse duration as well the smooth temporal behaviour. The smooth temporal behaviour of the irradiated power, without any spikes, prevents the undesired material ablation.

The penetration depth of the energy deposition is negligible for the laser ($\approx 17 \text{ nm}$), similar to the case of fusion devices and is always small in comparison to the temperature decay length at the end of the laser pulse. Thus the heat load technique based on high energy lasers is an excellent method for the simulation of the effect of ELM-like heat loads under laboratory conditions.

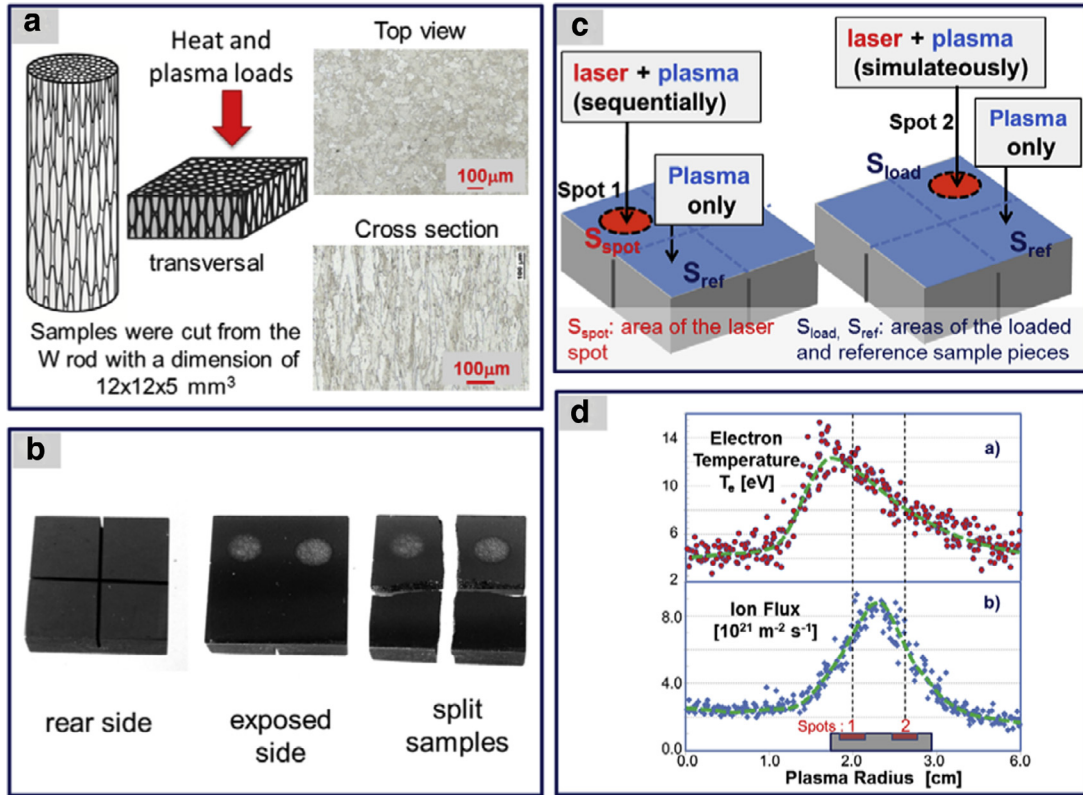


Fig. 2. (a) The microstructure of an ITER-like tungsten sample: top view and cross section, (b) castellated tungsten sample composed of four sections separated by narrow grooves of ~ 0.3 mm, (c) experimental scheme for the combined test of one W sample in PSI-2, and (d) electron temperature and ion flux radial profiles at PSI-2.

All tungsten samples with dimensions of $12 \times 12 \times 5$ mm³ were cut by electrical discharge machining (EDM) from tungsten rod and afterwards mechanically polished to the mirror-like finish with a roughness R_a of less than $0.1 \mu\text{m}$ and cleaned in an ultrasonic bath. They were then outgassed at $\approx 1000^\circ\text{C}$ under vacuum for several hours prior to the exposure.

The tungsten material with a purity of 99.5 wt% was produced by powder metallurgical routes at Plansee SE [12] and fulfils the ITER-grade specification. The grains of the tungsten specimens were oriented perpendicularly (transversally) to the loaded surface with a typical grain length around $110 \mu\text{m}$ and width of about $40 \mu\text{m}$ (see Fig. 2a). Each sample is castellated (see Fig. 2b), i.e. composed of four sections separated by narrow grooves (~ 0.3 mm). This castellation allows easy splitting of the sample into 4 pieces without increase of their temperatures, keeping the D-inventory unchanged. Each of the pieces contains only a single laser spot (or none if it is used for reference).

The experiment is carried out as follows. Firstly, only an area of piece 1 was exposed to laser pulses. After that, all four pieces were exposed to the plasma with simultaneous ELM-like transient heat loads by laser onto piece 2 (Fig. 2 c). The reference pieces 3 and 4 are located on the same plasma radius as pieces 2 and 1 and were correspondingly exposed to the same ion flux (Fig. 2 d).

After laser irradiation, the induced surface modifications on all samples were investigated by laser profilometry, optical microscopy and scanning electron microscopy (SEM). In addition the cross sections were examined by metallographic means to analyse the crack propagation into the bulk material. The deuterium inventory in the near surface region (down to $4.4 \mu\text{m}$) of the samples was measured by nuclear reaction analysis (NRA) with help of the $\text{D}(^3\text{He}, \alpha)\text{p}$ nuclear reaction on the laser spot locations and corresponding reference locations. The ^3He 3 MeV beam of NRA has a diameter of about 1 mm and was positioned at the centre of the

laser spot. Finally, the target was split in 4 pieces after which the deuterium content in each piece was measured with help of thermal desorption spectroscopy (TDS). The samples were heated with slow temperature ramps of ~ 0.35 K/s to 1273 K. During heating the, H_2 (mass 2) HD (mass 3), D_2 (mass 4) molecules were recorded by a calibrated quadrupole mass spectrometer. To compare local NRA measurements and total number of desorbed D atoms from the pieces measured by TDS, the surface density of D atoms [C_D] inside the laser spot has been evaluated from the TDS data (applied to the laser exposed and the reference pieces, the latter only exposed to D-plasma) by the following equation:

$$C_D [\text{at}/\text{m}^2] = \left(D^{\text{load}} - \frac{D^{\text{ref}}}{S_{\text{ref}}} \times (S_{\text{load}} - S_{\text{spot}}) \right) / S_{\text{spot}}$$

where D^{load} and D^{ref} are the total amount of deuterium desorbed by TDS respectively from laser loaded and reference pieces, S_{load} and S_{ref} are the areas of laser loaded and reference pieces and S_{spot} is the area of the laser spot. (see Fig. 2c).

3. Result and discussion

The choice of the base temperature of the investigated W samples in our experiments is the important issue to avoid altering the D retention only due the excursion of the base temperature during the laser exposure. Before thermal shock exposure the base temperature of the investigated W samples was around room temperature (RT) and the temperature excursion during the pulsed irradiation is expected to exceed the ductile-to-brittle transition temperature (DBTT) of ~ 500 to 700 K [13]. The base temperature of the test samples, mounted on an actively cooled target holder, increased during the combined laser and plasma exposures by 130 K at most.

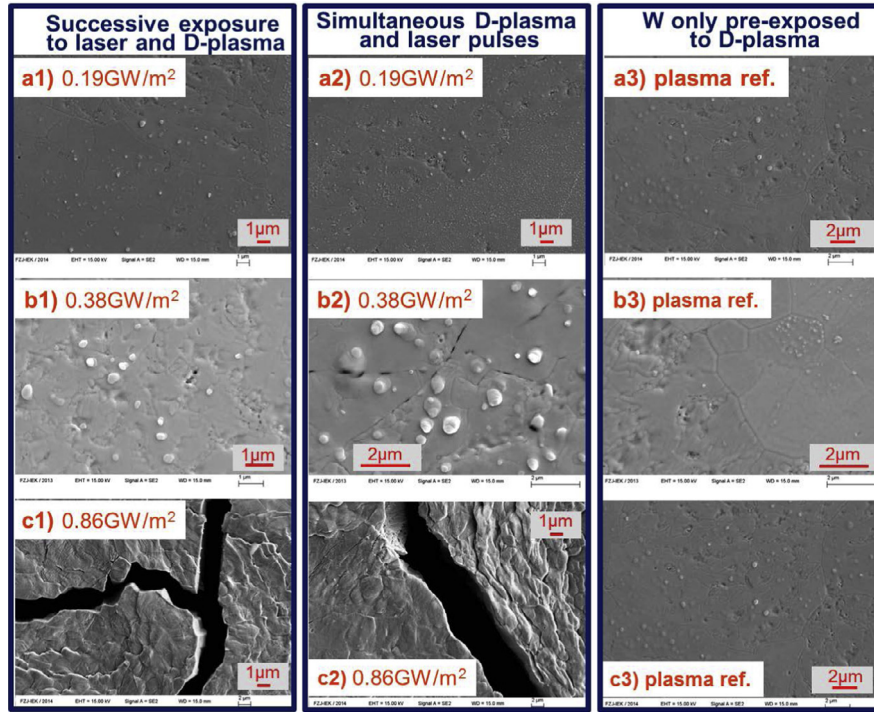


Fig. 3. SEM micrographs of an ITER-like tungsten exposed each to 1000 laser pulses for a power density range between 0.19 GW/m^2 and 0.86 GW/m^2 (a1, b1 and c1) after successive exposure of tungsten to transient heat loads and deuterium plasma (a2, b2 and c2) after simultaneous exposure to transient heat loads and to D plasma (a3, b3 and c3) after pure D loading at PSI-2 at a fluence of $1.2 \times 10^{25} \text{ m}^{-2}$ (ion fluxes of $6.0 \times 10^{21} \text{ m}^{-2} \text{ s}^{-1}$ for a time period of 2000 s) and incident ion energy of 60 eV.

Previous investigations discover the temperature dependence of the D retention in tungsten with a maximum at 500–700 K [14–16]. In the temperature range from RT to roughly 500 K however, no or a weak dependence of the retention on temperature has been observed. Additionally, there is a fluence dependence of retention as well as the dependence of retention on different tungsten grades [17]. In this contribution, the sample temperature increased during the plasma exposure up to 130–150 K even after 10,000 pulses at maximal exposed laser power of $P_{\text{las}} = 0.86 \text{ GW/m}^2$. The major contribution to this increase is due to plasma exposure. If we assume that the both sections are fully thermally isolated, the expected maximal difference between the laser exposed and reference sample is about 30 K. However, the sections are not thermally isolated and thus both sections have nearly the same temperature or at least smaller temperature differences. Thus we can conclude that the expected retention altering is due to the impact of the transient heat loads and not due to the increase of the basis temperature between the pulses.

3.1. Surface morphology of tungsten after combined deuterium plasma and transient heat load exposure

Low-energy hydrogen-isotopes plasma exposure in combination with the transient heat loads could induce strong surface modifications caused by impact of transient heat loads as well as by the implantation of hydrogen isotopes from the plasma.

The successive and simultaneous exposure of ITER-like tungsten was performed at three different laser power densities, 0.19 GW/m^2 , 0.38 GW/m^2 and 0.86 GW/m^2 as shown in Fig. 3. Each of these samples has been exposed each to 1000 laser pulses at pulse duration of 1 ms and a repetition rate of 0.5 Hz. Thus, the laser power density range in our experiment was chosen so that we could investigate the impact of the transient heat loads on the fuel retention of tungsten for the power densities below (Fig. 3a1–a3) and beyond the damage threshold for the W (Fig. 3c1–c3 the sample exposed to power of 0.86 GW/m^2 exhibits strong crack for-

mation). At the same time the power densities used in the current work are similar to those expected during type-I ELM events in ITER [18,10].

Low-energy hydrogen-isotopes plasma exposure in combination with the transient heat loads could induce strong surface modifications caused by strong heat loads as well as by the implantation of hydrogen isotopes from the plasma. Surface modifications were investigated with a scanning electron microscope (SEM) at the sample which coincides with the maximum of plasma flux density. Fig. 3 shows SEM images taken after successive exposure of tungsten to transient heat loads and deuterium plasma (a1, b1 and c1) and after simultaneous exposure to transient heat loads and to D plasma (a2, b2 and c2) and as well as after pure D loading (a3, b3 and c3) at PSI-2 at a fluence of $1.2 \times 10^{25} \text{ m}^{-2}$ (ion fluxes of $6.0 \times 10^{21} \text{ m}^{-2} \text{ s}^{-1}$ for a time period of 2000 s) and incident ion energy of 60 eV. The base temperature of the W samples before thermal shock exposure was around room temperature (RT).

In addition, intrinsic defects such as dislocations and vacancies could also act as trapping centres for deuterium and lead to bubble nucleation [19–21], so-called blisters (gas-filled bubbles and cavities). Enhanced blister formation of larger sizes up to $2.0 \mu\text{m}$ has been observed in the experiment with deuterium loading and simultaneous laser exposure at powers around the damage threshold 0.38 GW/m^2 (Fig. 3b2). The exposures with lower (Fig. 3a2) and higher power (Fig. 3c2) densities show the formation of blisters with much smaller sizes as well with the reduced density numbers. In contrast to the simultaneous plasma and laser exposure they are smaller ($0.3 \mu\text{m}$) (Fig. 3a1, b1 and c1) at the successive exposure of tungsten to transient heat loads and to the deuterium plasma. Very little blister formation and much smaller sizes (Fig. 3a3, b3, and c3), has been observed for samples which were exposed to the pure plasma loading. The blister formation has been verified by EDX measurements to exclude the deposition of material droplets on the surface and by FIB cross sections, which clearly showed the formation of small cavities below the surface [22].

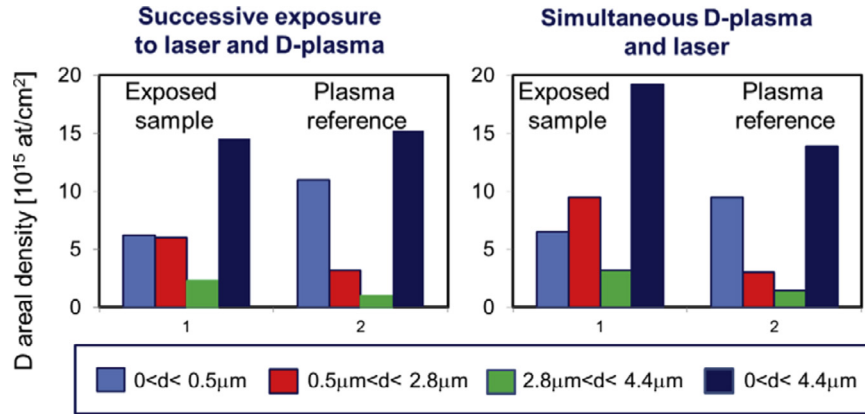


Fig. 4. Amount of D retained in the near surface region of tungsten specimen at sample base sample temperature of ≈ 300 K as determined by NRA. Left hand side: After successive exposure of tungsten to transient heat loads and deuterium plasma; right hand side: after at a combined laser heat loads and steady-state plasma exposure. The laser power density was 0.86 GW/m^2 with a pulse duration of 1 ms and the number of applied pulses amounted to 1000 at a repetition rate of 0.5 Hz.

The blisters are irregularly distributed over the sample surface with a tendency to form groups. The observed blisters with sizes much smaller than the width of the grain ($40 \mu\text{m}$) appear with a large number density on certain grains whereas on others they are completely absent. This behaviour has been observed in the previous experiment [23] and this is probably related to the crystallographic orientation [24].

Blistering at tungsten surfaces in fusion devices may result in instability of the plasma due to high-Z impurity release into the core plasma and sudden gas recycling if blisters burst eject large amounts of gas and/or material from the blister cap [25]. In addition, an increasing inventory of hydrogen isotopes in the near-surface region of the plasma-facing components, particularly of the radioactive fusion fuel tritium, will result in great concerns with respect to safety and cost efficiency [26]. Later in this work we will show that only 34% of the retained deuterium is located inside the near-surface layer ($d < 4 \mu\text{m}$) and blisters are not mainly responsible for the pronounced increase of the D retention. These results are fully consistent with the previous observation in [27] reporting that only 3–5% of the total D amount is retained in the blisters.

3.2. The impact of the transient heat cycling loads on the fuel retention in tungsten

3.2.1. NRA depth profiles of D retained in the near-surface of the tungsten samples after the transient heat cycling loads

Fig. 4 shows NRA depth profiles of D retained in W samples after successive exposure of tungsten to transient heat loads and deuterium plasma (left hand side) as well as after a combined laser heat load and steady-state plasma exposure (right hand side) at a sample base sample temperature of ≈ 300 K. The measurements have been carried out by means of NRA using a $2.94 \text{ MeV } ^3\text{He}^+$ beam at the centre of the laser spot. Under these conditions, the information depth in the tungsten material is limited to about $4.4 \mu\text{m}$. The NRA spectra are acquired using two partially depleted silicon detectors with thicknesses of $300 \mu\text{m}$ and $1500 \mu\text{m}$ respectively. The thick detector is equipped with a $10 \mu\text{m}$ Al foil to allow the high count rates of the protons released from the $\text{D}(^3\text{He}, \text{p})^4\text{He}$ reaction. The spectra are analysed with the SimNRA 6.06 software [28]. The depth information is determined in 3 depth bins, maintaining more than 100 counts in each bin and keeping the bins larger in depth span than the depth resolution of the corresponding reaction as determined by spectrum simulation code RESOL-NRA [29].

The deuterium depth distributions determined for the reference sample pieces show a high deuterium concentration in

a very narrow region close to the sample surface ($d < 0.5 \mu\text{m}$): about 72% of the total amount of D is retained in the $4.4 \mu\text{m}$ surface layer. Deeper into the bulk of the sample, the deuterium content decays strongly as can be seen in Fig. 4: about $11 \times 10^{15} \text{ at/cm}^2$ in the region close to the surface ($0 < d < 0.5 \mu\text{m}$), $3.2 \times 10^{15} \text{ at/cm}^2$ and $1.0 \times 10^{15} \text{ at/cm}^2$ in the regions $0.5 < d < 2.8 \mu\text{m}$ and $2.8 < d < 4.4 \mu\text{m}$ correspondingly.

The amount of D retained in the $4.4 \mu\text{m}$ surface layer, $14.5 \div 15.0 \times 10^{15} \text{ at/cm}^2$, has not been changed after successive exposure to laser and D-plasma. Here we should explicitly bring to attention that this statement refers to D-concentration inside the $4.4 \mu\text{m}$ layer only which not reflects the total amount in the bulk. Unfortunately, the TDS data, which provide the total amount of D, for this sample with $P_{\text{las}} = 0.86 \text{ GW/m}^2$ are not available due to failure of the RGA detector during the TDS measurements. The measurements by the NRA and TDS will be discussed later in the paragraph 3.2.2.

The deuterium concentration in a narrow region below $0.5 \mu\text{m}$ decreases and the D content in the region of $0.5 < d < 2.8 \mu\text{m}$ rises. In these experiments, the laser power density was $P_{\text{las}} = 0.86 \text{ GW/m}^2$ at pulse duration of 1 ms and the number of applied pulses amounted to 1000 at a repetition rate of 0.5 Hz.

The simultaneous transient heat loads and plasma exposure show increased total amount of D retained in the $4.4 \mu\text{m}$ surface layer as well as an influence on the depth profile of the deuterium. The total amount of the D concentration inside the $4.4 \mu\text{m}$ layer increased from $13.9 \times 10^{15} \text{ at/cm}^2$ to $19.2 \times 10^{15} \text{ at/cm}^2$. NRA depth profiling of the loaded tungsten revealed the peaking of the deuterium concentration in the region $0.5 < d < 2.8 \mu\text{m}$.

The power density dependence of the D content in the region close to the surface ($0 < d < 0.5 \mu\text{m}$) and the total amount of D in the surface layer below $4.4 \mu\text{m}$ are shown in Fig. 5 after successively (left hand side on the figure) and combined (right hand side on the figure) loadings. The D concentration has been normalised to the total amount of the deuterium in $4.4 \mu\text{m}$ of the reference tungsten surface layer ($C_d^{\text{laser}}/C_d^{\text{ref}}$). Both observed D content values decrease with power density in the experiment with W successively exposed to laser and D-plasma. For laser power densities beyond the 0.38 GW/m^2 the total content of deuterium of the $4.4 \mu\text{m}$ surface layer saturated and does not or weakly changed up to the 0.86 GW/m^2 . The NRA showed a strong increase of retention at the surface in the layer below $0.5 \mu\text{m}$ at power densities around 0.19 GW/m^2 which are significantly below the threshold for W damaging. (W sample exhibits a damage threshold between 0.38 GW/m^2 and 0.76 GW/m^2 for 1000 heat pulses [30].) Although the loads with powers below the damaging threshold do

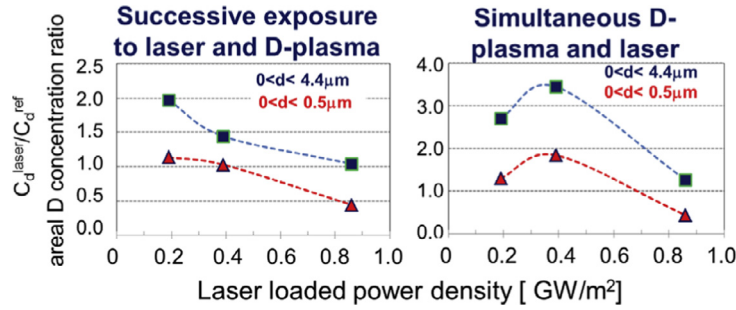


Fig. 5. Laser power density dependence of the deuterium retained inside the near-surface layers, $d < 0.5 \mu\text{m}$ and $d < 4 \mu\text{m}$, after successive exposure to laser and deuterium plasma.

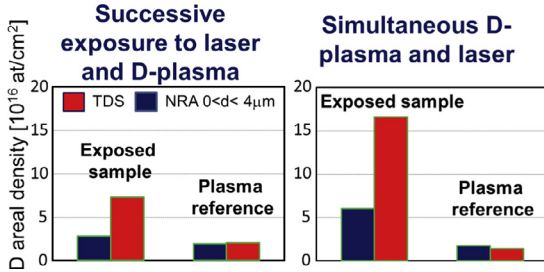


Fig. 6. Content of D retained in the near surface region of tungsten sample and the total amount of D as determined by NRA and TDS methods, correspondingly. The deposited energy density was fixed at 0.38 MJ m^{-2} and the number of laser pulses amounts to 1000 at a repetition rate of 0.5 Hz with the pulse width of 1 ms.

not lead to crack formation, they can lead to an enhanced accumulation of plastic deformation in the region close to the loaded surface and, correspondingly, to a higher concentration of defects and to higher D retention in this region.

The power density dependence of the D content in the experiments with combined exposure to D-plasma and laser (Fig. 5, right hand side) shows a maximum at the power density around the damage threshold 0.38 GW/m^2 . At larger laser powers the amount of the D-content inside the $4 \mu\text{m}$ layers looks similar to the reference samples.

One of the possible explanations of the similar deuterium amount inside the $4.4 \mu\text{m}$ near surface layer after pure D-plasma and successive exposures at larger laser power densities around 0.86 GW/m^2 could be that the numbers of defects inside the layer reduced due to recombination (so called annealing process), which is particularly intensive at higher material temperatures, as well as due migration/diffusion of defects during the laser exposure into the bulk.

This explanation could be applied also to the experiments with combined loading. Additionally to the successive exposures, the laser induced thermal desorption, which is used by the laser-induced desorption spectroscopy method [31], could play the significant role during the combined exposure at larger laser powers.

3.2.2. The impact of the transient heat cycling loads on the total amount of D retained in the W samples

Fig. 6 shows the results of TDS and NRA measurements of the D content in the W samples after successive exposure of tungsten to transient heat loads and deuterium plasma (left hand side) as well as after simultaneous exposure to the D-plasma and laser (right hand side). In these experiments, the deposited energy density was fixed at 0.38 MJ m^{-2} and the number of laser pulses amounts to 1000 at a repetition rate of 0.5 Hz with the pulse width of 1 ms. The specimens were exposed to high-flux deuterium plasma at base temperature of $\approx 300 \text{ K}$ before thermal shock as well as be-

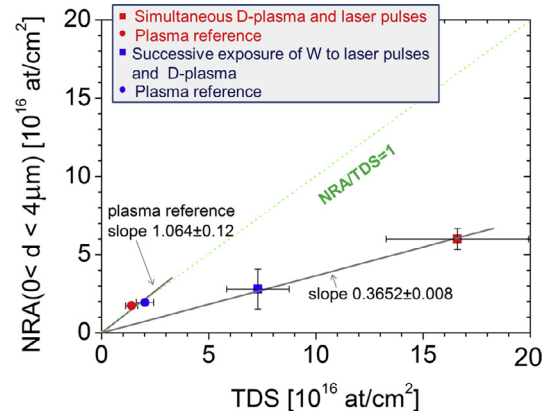


Fig. 7. D-content in the near-surface layer delivered by NRA method as function of the total D-inventory measured by TDS analysis. Tungsten sample was exposed to 1000 laser pulses for a power density of 0.38 GW/m^2 .

fore plasma. However it increases continuously with loading exposure time and reaches the value of 350 K after 1000 laser pulses.

Fig. 6 confirms the findings during the experiment with power densities at 0.86 GW/m^2 that the sequence of the different loading types is of importance. After successive exposure to laser and D-plasma the total amount of D retained in the $4.4 \mu\text{m}$ surface layer kept unchanged. In contrast to this observation, synergistic effects under simultaneous loading conditions, lead to a significant impact on fuel retention in the PFCs. As opposed to the pure plasma loading the combined plasma and laser exposure shows maximal D-content stored in $4 \mu\text{m}$ near-surface layer: (a) $6 \times 10^{16} \text{ at/cm}^2$ with combined loading versus $1.74 \times 10^{16} \text{ at/cm}^2$ for the pure plasma loading (Fig. 6, right-hand side). The reference sample piece is located on the same plasma radius as loaded piece and, correspondingly, has the same ion flux.

TDS measurements demonstrate a pronounced increase in the D retention, more than a factor of 12, during the combined transient heat loads and plasma exposure. Also the experiment with successive exposure to transient heat loads and deuterium plasma shows the increased content of the D-atoms by more than a factor of 3.6 in comparison to the pure plasma loading. The deviation of the TDS and the NRA results for successive and combined exposure loadings indicating a deeper penetration of the D atoms in the W material.

Fig. 7 shows the D-content measured by NRA analysis as function of the D-content detected by the TDS method. The tungsten sample was exposed to 1000 laser pulses for a power density of 0.38 GW/m^2 . These experimental results show the linear dependence for successive and combined exposure loadings. The grey lines represent the linear least squares fits. The possible explanation of the observed linear dependence could be the similar shape

of the deuterium depth profiles after the successive and combined exposure loadings. For the pure plasma exposure experiments, the linear dependence has been expected because deuterium is retained mostly within 2.0 μm from the surface (see Fig. 4), which is covered by the measurement range of NRA, and correspondingly both analyses should show the same result. Despite the last fact, a systematic deviation by 6% (slope = 1.064) of the NRA and TDS results has been observed. Taking into account these systematic deviations, we could evaluate the fraction of the deuterium stored in the 4 μm near-surface layer ($0.3652/1.064 \approx 0.34$) which is about 34% for successive as well as for combined exposure loadings, confirming the previous statement about a deeper penetration of the D atoms in the W material.

A pronounced increase in the D retention during the simultaneous transient heat loads and plasma exposure indicates the enhanced hydrogen clustering by the thermal shock exposures, as seen on the increased blister size due to mobilisation and thermal production of defects during transients. The strong temperature gradients during the laser pulse exposure (maximal surface temperature of $T_{\text{surf}} \approx 1050 \text{ K}$ at 0.38 GW m^{-2} with 1 ms pulse duration) could also lead to the significant increase of the D retention during the combined loads due to increased diffusion of D-atoms into the W material and due to an increased mobility of D atoms along the shock-induced cracks.

It should be mentioned here, that the increase of the D retention might even be more pronounced when the transient heat loads will be accompanied, which is expected in ITER, by “an enhanced particle flux” during the ELM events.

4. Conclusions

The impact of combined high cycle ELM-like heat loads and steady state plasma exposure on the fuel retention in ITER-like tungsten has been studied in the linear device PSI-2 with the main objective of qualifying tungsten (W) as plasma-facing material.

Strong surface modifications have been investigated during the simultaneous and successive exposure of tungsten at laser power densities, P_{las} , of 0.19 GW/m^2 , 0.38 GW/m^2 and 0.86 GW/m^2 .

Enhanced blister formation of larger sizes up to 2.0 μm has been observed in the experiment with deuterium loading and simultaneous laser exposure at powers around the damage threshold 0.38 GW/m^2 . The exposures with lower and higher power densities show formation of blisters with much smaller sizes as well as with a reduced density number. Also the successive exposure of tungsten to transient heat loads and to the deuterium plasma demonstrates smaller blisters with sizes of $\approx 0.3 \mu\text{m}$. Furthermore, the pure plasma exposed samples showed less pronounced blister formation and much smaller sizes. It is shown that blisters are not the main responsible mechanism for the pronounced increase of the D retention.

The experiment with laser and plasma exposures shows that the sequence of these exposures has a significant influence on the fuel retention in the near-surface region of W as well as on the depth profile of the deuterium:

Pure D-plasma exposure: a high deuterium concentration in a narrow region close to the sample surface ($d < 0.5 \mu\text{m}$) that is about 72% of the total amount of D retained in the 4.4 μm surface layer. Deeper into the bulk of the sample, the deuterium content decays strongly.

After successive exposure to laser and D-plasma: the total amount of retained D in the 4.4 μm surface layer has not been changed. Significant changes in the depth profile have been observed.

Simultaneous transient heat loads and plasma exposure: significant impact on the total amount of D retained in the 4.4 μm surface layer as well as on the depth profile of the deuterium. The total amount of the D concentration in this layer increases by $\approx 40\%$.

NRA depth profiling of the loaded tungsten exhibited a peak of the deuterium concentration in the region $0.5 < d < 2.8 \mu\text{m}$.

The experiment shows that, under simultaneous loading conditions, synergistic effects lead to a significant impact on the total fuel retention as measured by TDS. An increase of more than a factor of 12 has been observed during the simultaneous transient heat loads ($P_{\text{las}} = 0.38 \text{ GW/m}^2$) and plasma exposure. Successive exposure to transient heat loads ($P_{\text{las}} = 0.38 \text{ GW/m}^2$) and deuterium plasma also shows an increased content of D-atoms, by more than a factor of 3.6, in comparison to the pure plasma loading. These experimental findings for both simultaneous and sequential exposures to laser indicate enhanced hydrogen clustering due to the thermal shock exposures, as seen on the increased blister size due to mobilisation and thermal production of defects during transients. In addition, the significant increase of D retention during the simultaneous loads could be explained by an increased diffusion of D atoms into the W material due to strong temperature gradients during the laser pulse exposure (maximal surface temperature of $T_{\text{surf}} \approx 1050 \text{ K}$ at $P_{\text{las}} = 0.38 \text{ GW m}^{-2}$ with 1 ms pulse duration) and to an increased mobility of D atoms along the shock-induced cracks.

Combined measurements by NRA and TDS of the amount of D retained in the samples shows that only 34% of D is stored in a 4 μm thick, near-surface layer in tungsten after transient heat load cycling.

Acknowledgements

This work has been carried out within the framework of the EUROfusion Consortium and has received funding from the Euratom Research and Training Programme 2014–2018 under Grant agreement no. 633053. The views and opinions expressed herein do not necessarily reflect those of the European Commission. This work was financially supported by the Ministry of Education and Science of the Russian Federation.

References

- [1] 13th ITER Council, 20–21 November 2013.
- [2] R.A. Pitts, S. Carpentier, F. Escourbiac, et al., J. Nucl. Mater. 438 (2013) 48–56.
- [3] G. Janeschitz, ITER JCT and HTs, J. Nucl. Mater. 290–293 (2001) 1.
- [4] H.D.B. Jenkins, H.K. Roobottom, CRC Handbook of Chemistry and Physics, 85th ed., CRC Press, Boca Raton, FL, 2004.
- [5] T. Hirai, et al., Phys. Scr. T103 (2003) 59.
- [6] O. Ogorodnikova, et al., J. Nucl. Mater. 313–316 (2003) 469.
- [7] G. De Temmerman, J.J. Zielinski, S. Van Diepen, L. Marot, M. Price, Nucl. Fusion 51 (2011) 073008.
- [8] K.R. Umstadter, R. Doerner, G. Tynan, J. Nucl. Mater. 386–388 (2009) 751–755.
- [9] M. Wirtz, J. Linke, G. Pintsuk, G. De Temmerman, G.M. Wright, J. Nucl. Mater. 443 (2013) 497–501.
- [10] A. Loarte, B. Lipschultz, A.S. Kukushkin, et al., Progress in the ITER physics basis, Nucl. Fusion 47 (2007) 203.
- [11] A. Kreter, C. Brandt, A. Huber, et al., Fusion Sci. Technol. 68 (1) (2015) 8–14.
- [12] Plansee Group Homepage 2012. <http://www.plansee.com/de/index.htm>.
- [13] J.W. Davis, et al., J. Nucl. Mater. 258–263 (1998) 308.
- [14] V.Kh. Alimov, W.M. Shu, J. Roth, et al., Phys. Scr. T138 (2009) 014048–1–014048–5.
- [15] M.J. Baldwin, R.P. Doerner, W.R. Wampler, et al., Nucl. Fusion 51 (2011) 103021–1–103021–9.
- [16] V.Kh. Alimov, W.M. Shu, J. Roth, et al., J. Nucl. Mater. 417 (2011) 572–575.
- [17] O.V. Ogorodnikova, T. Schwarz-Selinger, K. Sugiyama, Phys. Scr. T138 (2009) 014053–1–014053–5.
- [18] G. Federici, A. Loarte, G. Strohmayer, Plasma Phys. Control. Fusion 45 (2003) 1523.
- [19] H.B. Zhou, Y.L. Liu, S. Jin, et al., J. Nucl. Fusion 50 (2010) 025016.
- [20] O. Ogorodnikova, J. Roth, M. Mayer, J. Nucl. Mater. 373 (2008) 254–258.
- [21] A.A. Haasz, M. Poon, R.G. Macaulay-Newcombe, J.W. Davis, et al., J. Nucl. Mater. 290 (2001) 85–88.
- [22] M. Wirtz, S. Bardin, A. Huber, et al., Nucl. Fusion 55 (2015) 123017 9pp, doi:10.1088/0029-5515/55/12/123017.
- [23] M.H.J. t’Hoen, M. Balden, A. Manhard, et al., Nucl. Fusion 54 (2014) 083014–1–083014–10.
- [24] H.Y. Xu, Y.B. Zhang, Y. Yuan, et al., J. Nucl. Mater. 443 (2013) 452.
- [25] W.M. Shu, E. Wakai, T. Yamanishi, Nucl. Fusion 47 (2007) 201.

- [26] J. Roth, E. Tsitrone, T. Loarer, et al., *Plasma Phys. Control. Fusion* 50 (2008) 103001-1–103001-20.
- [27] A. Manhard, U.V. Toussaint, T. Dürbeck, et al., *Phys. Scr.* T145 (2011) 014038-1–014038-4.
- [28] M. Mayer, SimNRA User's Guide, Technical Report IPP 9/113, Max-Planck-Institut für Plasmaphysik, Garching, 1997.
- [29] M. Mayer, *Nucl. Instrum. Methods B* 266 (2008) 1852.
- [30] A. Huber, A. Arakcheev, G. Sergienko, I. Steudel, M. Wirtz, et al., *Phys. Scr.* T159 (2014) 014005, doi:[10.1088/0031-8949/2014/T159/014005](https://doi.org/10.1088/0031-8949/2014/T159/014005).
- [31] M. Zlobinski, V. Philipps, B. Schweer, A. Huber, et al., *J. Nucl. Mater.* 438 (2013) 1155.